



Free Vibration Analysis of an Axially Functionally Graded Rotating Tapered Rayleigh Beam Using Differential Transform and Variational Iteration Methods

¹Olotu, O.T., ²Agboola, O.O., ¹Gbadeyan, J.A., *¹Adeniran, P.O., & ³Akinremi, J.O.

¹Department of Mathematics, University of Ilorin, Ilorin, Kwara State, Nigeria

²Department of Mathematics, Covenant University, Ota, Ogun State, Nigeria

³Department of Physical Sciences/Computing Sciences, Hillside University of Science and Technology, Okemesi, Ekiti State, Nigeria

*Corresponding author email: femiadeniran92@gmail.com

Abstract

The free vibration response of an axially functionally graded rotating cantilever tapered Rayleigh beam based on Rayleigh Beam Theory (RBT) is studied using the Differential Transform Method (DTM) and Variational Iteration Method (VIM). Firstly, the governing partial differential equations of motion are simplified into ordinary differential equations through the separation of variables. Then, dimensionless parameters are integrated into the equations of motion to derive a set of recurrence equations. Utilising MAPLE 18 computer codes, the dimensionless frequencies and mode shapes are computed through direct algebraic operations and derived equations. The competency of DTM and VIM in determining the frequency parameters and the vibration modes of a rotating cantilever tapered Rayleigh beam composed of gradient materials is examined, and the influences of taper ratio, inverse of the slenderness ratio and rotational speed on the dimensionless frequencies are analysed. The first eight dimensionless frequencies' convergence and the associated vibration modes are displayed in graphs. For validation of results, a comparison is carried out between the methods adopted in this study. The outcomes reveal that the two semi-analytical techniques are effective and reliable and can be easily employed to examine functionally graded beams' free vibration. The results obtained show that there is excellent agreement between the two methods used.

Keywords: Rotating Tapered Beam, Free Vibration, Functionally Graded Beam, Variational Iteration Method, Differential Transform Method

Introduction

An entirely modern family of hybrid materials called Functionally Graded Materials (FGMs), is studied in this work. In the past few years, the stationary and kinetic examination of Functionally Graded Beams (FGBs) has significantly drawn a large number of researchers. The concept of materials with functional grades was first proposed in 1984 by experts from various disciplines in Japan as means of creating heat-resistant materials (Nguyen et al., 2020). The research on FGMs is increasing exponentially due to its capability to meet some expected material features unlike the usual non-heterogeneous and layered composite materials which undergo separation between them, massive residual stress, immense plastic distortions, etc. A FGM can be suitable alternative for structural materials of rotating beams since the dynamic behaviour of engineering components with FGMs plays a vital role in both research as well as industrial fields. Several investigations have been performed on functionally graded materials. New heterogeneous materials that are functionally graded are employed to design structures when exposed to high temperatures. FGMs are metal-matrix composites characterized by gradual changes in material ratios. Typically, these materials consist of ceramic and metal alloy blended together or from materials integration. The ceramic component is responsible for the high-thermal resilience as result of its low heat conductivity. Functionally graded materials are one of the high-tech materials whose physical-mechanical parameters vary continuously with respect to position or distance. The usage of FGMs in load-bearing structures leads stress relief, improves the strength and toughness of structure. The deformable metal component however, prevents breakage caused by stresses as a result of rapid temperature change in a short time frame. FGMs have

become increasingly useful and are now being applied in high-tech transportations and defense industries, nuclear reactors and electronics.

Ebrahimi and Dashti (2015) used DTM in a study to examine the free vibration response of a spinning double tapered FGB in which the material parameters of the beam gradually change throughout the thickness in line with the power-law distribution in the proportion of constituent volumes. The study on free vibration of simply supported Rayleigh beam made up of multiphase materials was carried out by Avcar and Alwan, (2007) in which the equations describing the dynamics of FGBs were determined based on Rayleigh beam theory and the beam's material parameters are steadily graded throughout its thickness in accordance with power-law distribution. The formulation of a detailed transfer matrix technique for investigating the natural vibration properties of a FGB whereby the transfer matrix for the composite beam was derived from the interaction between forces and displacements at both beam ends (Lee, 2017). A novel technique to natural vibration properties of FG rotating Bernoulli-Euler beam using DTM was investigated by (Kumar et al., 2017). An overview of the dynamic stiffness method (DSM) for natural vibration characteristics of both functionally and non functionally graded beams in which the Wittrick-Williams algorithm was adopted to demonstrate the effectiveness of DSM in addressing free vibration problem of beams was presented by (Banerjee, 2019). The analysis of dynamic behaviour of spinning Timoshenko beams made up of axially graded materials that undergone flapwise bending using differential transform method was examined by (Ozdemir, 2019). The dynamic equilibrium and natural vibration properties of a spinning FG Timoshenko beam with gradual material property variations along its thickness in line with the power and exponential rules using finite element method was conducted by (Padhi et al., 2019).

Different approaches, theories and assumptions have been employed in numerous researches to examine how functionally graded beams behave dynamically when subjected to different transient loads system (Al-Hawamdeh et al., 2017; Abu-Alshaiikh & Almbaidin, 2020; Akbas, 2020; Huang et al., 2023; Nguyen et al., 2020). Gbadeyan and Olotu, (2020) examined the natural vibration study of rotating non-uniform prestressed Rayleigh beam via DTM whereby, they considered a model for which only the mass density per unit length remains constant while the modulus of elasticity was a function of coordinate x . Investigation was carried out on the dynamic reactions of beams in rotation with elastic constraints utilizing the modified Fourier series method, revealing the significant influence of linear springs on frequency and the lagging effect of elastic restraints on the rotational speed, as stated by (Guo et al., 2024; Wang et al., 2022). The finite element technique was used to examine how rotational speed affected a spinning cantilever beam's vibration. According to Ilechukwu et al. (2024), this study illustrated significance of taking rotational effects into account when designing beams. Non-uniform Rayleigh beams' dynamic behaviour in free vibration with a clamped-free boundary condition under rotation was examined, highlighting the superiority of p-FEM over h-FEM through convergence studies (Dhar & Sakar, 2023). The modeling and vibration behaviour of rotating piezoelectric multi-layer beams were investigated in a study by Chen et al. (2024), which found that the modal characteristics were significantly influenced by the tip mass, setting angle, and rotating speed.

The free dynamic response of double-tapered beams in rotation which comprised of two-way functionally graded materials was conducted using three different beam theories, (Taima et al., 2023). An investigational research was conducted to analyze the flap-wise dynamic characteristics of spinning beams with varied cross-sectional designs. Digital Image Correlation measurement and Frequency Domain Decomposition were employed to find the vibration characteristics of the system (Huang et al., 2023). In order to give useful analytical approximations for structural design projects, a study examined the vibration behaviour of non-uniform beams using the Aboodh transform-based variational iteration method (Anjum et al., 2024). Addressing a critical knowledge gap in vibration analysis, this study focuses on analyzing the natural vibration properties of axially FG tapered rotating cantilever Rayleigh beams, a problem that has not been adequately addressed despite extensive research on FG beams. In order close this gap, the study uses two numerical techniques to examine the beam's free vibration - the VIM and DTM. The gradient material properties-the mass density and the modulus of elasticity are assumed to exhibit a continuous variation through the beam's axial length. This study contributes to filling the knowledge gap in the vibration behaviour of FG beams, specifically for axially FG tapered rotating cantilever Rayleigh beams. The findings will provide valuable insights for researchers and engineers working on similar problems.

Materials and methods

Considering an axially functionally graded rotating cantilever tapered Rayleigh beam about a vertical axis with a uniform rotation speed Ω of finite length l as shown in Figure 1. The governing equation of motion is given by (Li et al., 2015) as

$$\frac{\partial^2}{\partial x^2} \left[E(x)I(x) \frac{\partial^2 M(x,t)}{\partial x^2} \right] + \rho(x)A(x) \frac{\partial^2 M(x,t)}{\partial t^2} - \frac{\partial}{\partial x} \left[Q(x) \frac{\partial M(x,t)}{\partial x} \right] - \frac{\partial}{\partial x} \left[\rho(x)I(x) \frac{\partial^3 M(x,t)}{\partial x \partial t^2} \right] + \Omega^2 \frac{\partial}{\partial x} \left[\rho(x)I(x) \frac{\partial M(x,t)}{\partial x} \right] = 0, \quad x \in (0,l) \quad (1)$$

where $M(x, t)$ denotes the beam's dynamic response, $\rho(x)$ is the mass per unit volume, $I(x)$ is moment of inertia, $A(x)$ is the variable cross-sectional area, $E(x)$ is Young's modulus, x is the coordinate along the longitudinal axis, t is the time. $Q(x)$ is the arbitrary axial tensile excitation force. When an axial end force Q_0 is applied to the beam, $Q(x)$ is a constant function with $Q(x) = Q_0$. However, if the beam is impacted by distributed axial force $g(x)$, this implies that $Q(x) = \int_x^l g(\eta) d\eta$.

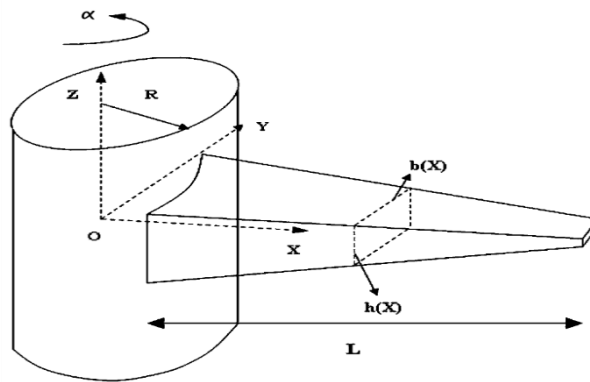


Figure 1: Configuration of axially functionally graded non-uniform rotating cantilever beam

The initial conditions are

$$M(x,0) = M_0(x) \quad \text{and} \quad \frac{\partial M(x,0)}{\partial t} = \dot{M}_0(x) \quad (2)$$

The boundary conditions are

At $x = 0$,

$$\frac{\partial M(x,t)}{\partial x} = 0 \quad (3)$$

$$M(x,t) = 0 \quad (4)$$

At $x = l$,

$$E(x)I(x) \frac{\partial^2 M(x,t)}{\partial x^2} = 0 \quad (5)$$

$$\frac{\partial}{\partial x} \left[E(x)I(x) \frac{\partial^2 M(x,t)}{\partial x^2} \right] - T(x) \frac{\partial M(x,t)}{\partial x} - \rho(x)I(x) \frac{\partial^3 M(x,t)}{\partial x \partial t^2} + \Omega^2 \rho(x)I(x) \frac{\partial M(x,t)}{\partial x} = 0 \quad (6)$$

For free vibration, the following form of response applies

$$M(x,t) = Y(x)(a_1 \cos \omega t + a_2 \sin \omega t) \quad (7)$$

Putting eq. (7) into eq. (1) leads to

$$\begin{aligned} \frac{d^2}{dx^2} \left[E(x)I(x) \frac{d^2 Y(x)}{dx^2} \right] - \rho(x)A(x)\omega^2 Y(x) - \frac{d}{dx} \left[Q(x) \frac{dY(x)}{dx} \right] + \frac{d}{dx} \left[\rho(x)I(x)\omega^2 \frac{dY(x)}{dx} \right] \\ + \Omega^2 \frac{d}{dx} \left[\rho(x)I(x) \frac{dY(x)}{dx} \right] = 0, \quad x \in (0,l) \end{aligned} \quad (8)$$

In addition, using eq. (7), eqs. (3) - (6) are stated as:

At $x = 0$

$$\frac{dY(x)}{dx} = 0 \quad (9)$$

$$Y(x) = 0 \quad (10)$$

At $x = l$,

$$E(x)I(x) \frac{d^2 Y(x)}{dx^2} = 0 \quad (11)$$

$$\frac{d}{dx} \left[E(x)I(x) \frac{d^2 Y(x)}{dx^2} \right] - \left[Q(x) - \rho(x)I(x)\omega^2 - \rho(x)I(x)\Omega^2 \right] \frac{dY(x)}{dx} = 0 \quad (12)$$

The dimensionless parameters are applied:

$$\left. \begin{aligned}
 \xi &= \frac{x}{l} & y(\xi) &= \frac{Y(x)}{l} \\
 v(\xi) &= \frac{E(x)I(x)}{E(0)I(0)} & q(\xi) &= -\frac{Q(x)l^2}{E(0)I(0)} \\
 p(\xi) &= \frac{\rho(x)A(x)}{\rho(0)A(0)} & \tau_J &= \frac{v'(\xi)}{v(\xi)} \Big|_{\xi=1} \\
 h(\xi) &= \frac{\rho(x)I(x)}{\rho(0)I(0)} & \eta_J &= \frac{T(l)l^2}{E(l)I(l)} \\
 \gamma &= \frac{1}{l} \sqrt{\frac{I(0)}{A(0)}} & \psi_J &= \frac{h(\xi)}{v(\xi)} \Big|_{\xi=1} \\
 \Lambda^2 &= \frac{\rho(0)A(0)\omega^2 l^4}{E(0)I(0)} & \alpha^2 &= \frac{\rho(0)A(0)\Omega^2 l^4}{E(0)I(0)}
 \end{aligned} \right\} \quad (13)$$

The dimensionless forms eq. (8) and eqs. (9) - (12) are expressed as:

$$\begin{aligned}
 &v(\xi) \frac{d^4 y(\xi)}{d\xi^4} + 2 \frac{dv(\xi)}{d\xi} \cdot \frac{d^3 y(\xi)}{d\xi^3} + \frac{d^2 v(\xi)}{d\xi^2} \cdot \frac{d^2 y(\xi)}{d\xi^2} + q(\xi) \frac{d^2 y(\xi)}{d\xi^2} + \frac{dq(\xi)}{d\xi} \cdot \frac{dy(\xi)}{d\xi} \\
 &+ \gamma^2 \left[h(\xi) \frac{d^2 y(\xi)}{d\xi^2} + \frac{dh(\xi)}{d\xi} \cdot \frac{dy(\xi)}{d\xi} \right] (\Lambda^2 + \alpha^2) - \Lambda^2 p(\xi) y(\xi) = 0 \quad (14)
 \end{aligned}$$

At $\xi = 0$,

$$\frac{dy(\xi)}{d\xi} = 0 \quad (15)$$

$$y(\xi) = 0 \quad (16)$$

At $\xi = 1$,

$$\frac{d^2 y(\xi)}{d\xi^2} = 0 \quad (17)$$

$$\frac{d^3 y(\xi)}{d\xi^3} + \tau_J \frac{d^2 y(\xi)}{d\xi^2} - \left[\eta_J - \Lambda^2 \gamma^2 \psi_J - \alpha^2 \gamma^2 \psi_J \right] \frac{dy(\xi)}{d\xi} = 0 \quad (18)$$

Differential Transform Method (DTM)

A reliable and analytical method is the Differential Transform Method (DTM) derived from Taylor series expansion, primarily used to solve differential equations. Introduced by Zhou in 1986, DTM effectively addresses both linear and nonlinear equations, particularly in the field of electrical circuits. Through specific transformation rules, DTM changes differential equations and their boundary conditions into algebraic equations. By solving these equations, the method yields the expected solutions. Unlike traditional high-order Taylor series expansions, that require symbolic manipulation of differential coefficients, DTM provides a recursive approach to obtain higher-order solutions. This process ultimately leads to an exact solution expressed in algebraic form. Basic definition and operations of DTM are presented as follows. Consider a function $y(t)$ that is analytic in the domain D . This function can be expressed as a power series expansion centered at any point in the domain. The differential transform of $y(t)$ is defined as:

$$\bar{Y}(n) = \frac{1}{n!} \left[\frac{d^n y(t)}{dt^n} \right]_{t=0} \quad (19)$$

In eq. (19), $y(t)$ is the original function and $\bar{Y}(n)$ is the transformed function.

The inverse differential transform of $\bar{Y}(n)$ is defined as

$$y(t) = \sum_{n=0}^{\infty} \bar{Y}(n) t^n \quad (20)$$

Combining eqs. (19) and (20) gives

$$y(t) = \sum_{n=0}^{\infty} \frac{t^n}{n!} \left[\frac{d^n y(t)}{dt^n} \right]_{t=0}, \quad (21)$$

denotes the Taylor series of $y(t)$ at $t = 0$. According to eq. (21) the Taylor series expansion is the source of the differential transformation concept. In practice, a finite series is used to define the function $y(t)$, and eq. (21) is written as

$$y(t) = \sum_{n=0}^m \bar{Y}(n) t^n \quad (22)$$

which implies that

$$y(t) = \sum_{n=m+1}^{\infty} \bar{Y}(n) t^n \quad (23)$$

is negligibly small.

The value of m in this study cannot be determined until the natural frequencies have converged.

In addition, the original functions are represented by the small letters and a bar over the capital letters to represent the functions that have been transformed.

Application of Differential Transform Method

Defining $\lambda = \Lambda^2$, the recursive algebraic relation holds when eq. (14) is differentially transformed:

$$\begin{aligned} & \sum_{\ell=0}^k \bar{V}(k-\ell)(\ell+1)(\ell+2)(\ell+3)(\ell+4)\bar{Y}(\ell+4) \\ & + 2 \sum_{\ell=0}^k (k-\ell+1)\bar{V}(k-\ell+1)(\ell+1)(\ell+2)(\ell+3)\bar{Y}(\ell+3) \\ & + \sum_{\ell=0}^k (k-\ell+1)(k-\ell+2)\bar{V}(k-\ell+2)(\ell+1)(\ell+2)\bar{Y}(\ell+2) \\ & + \sum_{\ell=0}^k \bar{Q}(k-\ell)(\ell+1)(\ell+2)\bar{Y}(\ell+2) + \sum_{\ell=0}^k (k-\ell+1)\bar{Q}(k-\ell+1)(\ell+1)\bar{Y}(\ell+1) \\ & + \gamma^2(\lambda + \alpha^2) \sum_{\ell=0}^k \bar{H}(k-\ell)(\ell+1)(\ell+2)\bar{Y}(\ell+2) \\ & + \gamma^2(\lambda + \alpha^2) \sum_{\ell=0}^k (k-\ell+1)\bar{H}(k-\ell+1)(\ell+1)\bar{Y}(\ell+1) = \lambda \sum_{\ell=0}^k \bar{P}(k-\ell)\bar{Y}(\ell) \end{aligned} \quad (24)$$

where $\bar{Q}(k)$, $\bar{P}(k)$, $\bar{Y}(k)$, $\bar{H}(k)$ and $\bar{V}(k)$ are the T-functions of $q(\xi)$, $p(\xi)$, $y(\xi)$, $h(\xi)$ and $v(\xi)$ respectively.

Eq. (19) is used to transform eqs. (15) and (16) into

At $\xi = 0$,

$$\bar{Y}(1) = 0 \quad (25)$$

and

$$\bar{Y}(0) = 0 \quad (26)$$

Eq. (20) is used to transform eqs. (17) and (18) into

At $\xi = 1$,

$$\sum_{k=0}^m k(k-1)\bar{Y}(k) = 0 \quad (27)$$

and

$$\sum_{k=0}^m k(k-1)(k-2)\bar{Y}(k) + \tau_j \sum_{k=0}^m k(k-1)\bar{Y}(k) - \left[\eta_j - \gamma^2(\lambda + \alpha^2)\psi_j \right] \sum_{k=0}^m k\bar{Y}(k) = 0 \quad (28)$$

Eqs. (25) - (28) are algebraic equations solved utilizing MAPLE 18.

Assumed that

$$\bar{Y}(2) = s \tag{29}$$

$$\bar{Y}(3) = z, \tag{30}$$

where s and z are undetermined constants. Putting $k = 0$ into eq. (24) yields

$$\bar{Y}(4) = - \left[\left(\frac{\bar{V}(2)}{6\bar{V}(0)} + \frac{\bar{Q}(0)}{12\bar{V}(0)} + \frac{\gamma^2(\lambda + \alpha^2)\bar{H}(0)}{12\bar{V}(0)} \right) s + \frac{\bar{V}(1)}{2\bar{V}(0)} z \right] \tag{31}$$

Similarly, putting $k = 1$ into eq. (24) to obtain

$$\bar{Y}(5) = \frac{1}{120} \left\{ \left(\frac{12\bar{V}(1)\bar{V}(2)}{\bar{V}^2(0)} + \frac{6\bar{V}(1)\bar{Q}(0)}{\bar{V}^2(0)} + \frac{6\gamma^2(\lambda + \alpha^2)\bar{V}(1)\bar{H}(0)}{\bar{V}^2(0)} - \frac{12\bar{V}(3)}{\bar{V}(0)} - \frac{4\bar{Q}(1)}{\bar{V}(0)} - \frac{4\gamma^2(\lambda + \alpha^2)\bar{H}(1)}{\bar{V}(0)} \right) s + \left(\frac{36\bar{V}^2(1)}{\bar{V}^2(0)} - \frac{36\bar{V}(2)}{\bar{V}(0)} - \frac{6\bar{Q}(0)}{\bar{V}(0)} - \frac{6\gamma^2(\lambda + \alpha^2)\bar{H}(0)}{\bar{V}(0)} \right) z \right\} \tag{32}$$

Using the same recurrence relation, the subsequent terms can be iteratively calculated, the m^{th} term $\bar{Y}(m)$ can also be determined, with m being a function of the dimensionless frequency's convergence. Putting $\bar{Y}(0)$ to $\bar{Y}(m)$ into eqs. (27) and (28) to get

$$b_{j1}^{(m)}(\lambda)s + b_{j2}^{(m)}(\lambda)z = 0, \quad j = 1, 2, \dots \tag{33}$$

where polynomials of λ that correspond to m are $b_{j1}^{(m)}(\lambda), b_{j2}^{(m)}(\lambda)$.

By eq. (33), we have the following frequency equation:

$$\begin{vmatrix} b_{11}^{(m)}(\lambda) & b_{12}^{(m)}(\lambda) \\ b_{21}^{(m)}(\lambda) & b_{22}^{(m)}(\lambda) \end{vmatrix} = 0 \tag{34}$$

The dimensionless frequencies are computed by solving eq. (34).

With $\lambda = \Lambda^2$, we get $\Lambda = \Lambda_i^{(m)}$, $i = 1, 2, \dots$ where $\Lambda_i^{(m)}$ is the i^{th} estimated dimensionless frequency that corresponds to m , given that m is established by applying the following preset value:

$$\left| \Lambda_i^{(m)} - \Lambda_i^{(m-1)} \right| \leq \delta \quad (35)$$

where $\Lambda_i^{(m-1)}$ is the i^{th} estimated dimensionless frequency that corresponds to $m - 1$ and ϵ is the error tolerance criterion. Thus, $\epsilon = 0.0001$ in this study. There is discussion of two cases from eq. (35).

CASE I: $\Lambda_i^{(m)}$ is the i^{th} estimated dimensionless frequency denoted Λ_i if eq. (35) is satisfied.

Putting Λ_i into eq. (33), gives

$$z = c_1 s \quad \text{where } c_1 \text{ is a constant.} \quad (36)$$

Putting Λ_i and eq. (36) into $\bar{Y}(0)$ to $\bar{Y}(m)$ using eq. (22), yields

$$y_i(\xi) = \sum_{k=0}^m \xi^k \bar{Y}^*(k) \quad (37)$$

given that $\bar{Y}^*(k)$ denotes $\bar{Y}(k)$ whose Λ and z are replaced by Λ_i and $c_1 s$, the i^{th} mode shape that corresponds to the dimensionless frequency Λ_i is $y_i(\xi)$. Additionally, by $\xi = \frac{x}{l}$ leads to

$$Y_i(x) = y_i\left(\frac{x}{l}\right) \quad (38)$$

CASE II: The procedures given below should be repeated until the i^{th} dimensionless frequency and i^{th} vibration mode are determined if eq. (35) is not satisfied.

Step 1: Replace m with $m + 1$.

Step 2: The identical procedure outlined in eqs. (34) - (38). The free vibration response can

be expressed using vibration mode functions as follows:

$$\phi(x, t) = \sum_{i=1}^{\infty} Y_i(x)(e_1 \cos \omega t + e_2 \sin \omega t), \quad (39)$$

where the initial conditions in eq. (2) determine e_1 and e_2 .

Variational Iteration Method (VIM)

Relatively few number of researchers has extensively used the VIM to solve vibration behaviour of structures. Since detailed information related to VIM is available in numerous literature, only basic concept of VIM is illustrated in this work .

Consider a general non-linear differential equation

$$L_y(\xi) + N_y(\xi) = f(\xi), \quad (40)$$

where $f(\xi)$ is a known continuous function, N and L are non-linear and linear operators, respectively. Using the VIM theory as a basis, the following correction functional was constructed.

$$y_{n+1}(\xi) = y_n(\xi) + \int_0^\xi \mu \{Ly_n(t) + Ny_n(t) - f(t)\} dt; n \geq 1, \quad (41)$$

Here, μ represents a generalized Lagrange multiplier derived from variational principle, $\tilde{y}_n(\xi)$ is a restricted variation of the nth-order approximation, which implies that $\delta \tilde{y}_n(\xi) = 0$ where δ is the variational derivative, $y_n(\xi)$ is the nth-order approximation for $y(\xi)$.

By making use of eq. (41), the correction functional for the dimensionless governing eq. (14) can be written as

$$y_{n+1}(\xi) = y_n(\xi) + \int_0^\xi \mu \left\{ y_n^{iv}(t) + 2 \frac{v'(t)}{v(t)} y_n'''(t) + \frac{v''(t)}{v(t)} y_n''(t) + \frac{q(t)}{v(t)} y_n'(t) + \frac{q'(t)}{v(t)} y_n(t) + \gamma^2 (\Lambda^2 + \alpha^2) \left[\frac{h(t)}{v(t)} y_n''(t) + \frac{h'(t)}{v(t)} y_n'(t) \right] - \Lambda^2 \frac{p(t)}{v(t)} y_n(t) \right\} dt \quad (42)$$

In this condition, the Lagrange multiplier (μ) can be determined as

$$\mu = \frac{(t - \xi)^3}{3!} \quad (43)$$

Putting eq. (43) into eq. (42) to give

$$y_{n+1}(\xi) = y_n(\xi) + \int_0^\xi \frac{(t - \xi)^3}{3!} \left\{ y_n^{iv}(t) + 2 \frac{v'(t)}{v(t)} y_n'''(t) + \frac{v''(t)}{v(t)} y_n''(t) + \frac{q(t)}{v(t)} y_n'(t) + \frac{q'(t)}{v(t)} y_n(t) + \gamma^2 (\Lambda^2 + \alpha^2) \left[\frac{h(t)}{v(t)} y_n''(t) + \frac{h'(t)}{v(t)} y_n'(t) \right] - \Lambda^2 \frac{p(t)}{v(t)} y_n(t) \right\} dt \quad (44)$$

If $n = 0, 1, 2, 3, \dots, k$, one can obtain the following successive iteration formula:

$$\begin{aligned}
 y_1(\xi) &= y_0(\xi) + \int_0^\xi \frac{(t-\xi)^3}{3!} \left\{ y_0^{iv}(t) + 2 \frac{v'(t)}{v(t)} y_0'''(t) + \frac{v''(t)}{v(t)} y_0''(t) + \frac{q(t)}{v(t)} y_0'' + \frac{q'(t)}{v(t)} y_0'(t) \right. \\
 &\quad \left. + \gamma^2 (\Lambda^2 + \alpha^2) \left[\frac{h(t)}{v(t)} y_0''(t) + \frac{h'(t)}{v(t)} y_0'(t) \right] - \Lambda^2 \frac{p(t)}{v(t)} y_0(t) \right\} dt \\
 y_2(\xi) &= y_1(\xi) + \int_0^\xi \frac{(t-\xi)^3}{3!} \left\{ y_1^{iv}(t) + 2 \frac{v'(t)}{v(t)} y_1'''(t) + \frac{v''(t)}{v(t)} y_1''(t) + \frac{q(t)}{v(t)} y_1''(t) + \frac{q'(t)}{v(t)} y_1'(t) \right. \\
 &\quad \left. + \gamma^2 (\Lambda^2 + \alpha^2) \left[\frac{h(t)}{v(t)} y_1''(t) + \frac{h'(t)}{v(t)} y_1'(t) \right] - \Lambda^2 \frac{p(t)}{v(t)} y_1(t) \right\} dt \\
 y_3(\xi) &= y_2(\xi) + \int_0^\xi \frac{(t-\xi)^3}{3!} \left\{ y_2^{iv}(t) + 2 \frac{v'(t)}{v(t)} y_2'''(t) + \frac{v''(t)}{v(t)} y_2''(t) + \frac{q(t)}{v(t)} y_2''(t) + \frac{q'(t)}{v(t)} y_2'(t) \right. \\
 &\quad \left. + \gamma^2 (\Lambda^2 + \alpha^2) \left[\frac{h(t)}{v(t)} y_2''(t) + \frac{h'(t)}{v(t)} y_2'(t) \right] - \Lambda^2 \frac{p(t)}{v(t)} y_2(t) \right\} dt \\
 &\quad \vdots \quad \quad \quad \vdots \quad \quad \quad \vdots \\
 &\quad \vdots \quad \quad \quad \vdots \quad \quad \quad \vdots \\
 &\quad \vdots \quad \quad \quad \vdots \quad \quad \quad \vdots
 \end{aligned}$$

$$\begin{aligned}
 y_k(\xi) &= y_{k-1}(\xi) + \int_0^\xi \frac{(t-\xi)^3}{3!} \left\{ y_{k-1}^{iv}(t) + 2 \frac{v'(t)}{v(t)} y_{k-1}'''(t) + \frac{v''(t)}{v(t)} y_{k-1}''(t) + \frac{q(t)}{v(t)} y_{k-1}'' + \frac{q'(t)}{v(t)} y_{k-1}'(t) \right. \\
 &\quad \left. + \gamma^2 (\Lambda^2 + \alpha^2) \left[\frac{h(t)}{v(t)} y_{k-1}''(t) + \frac{h'(t)}{v(t)} y_{k-1}'(t) \right] - \Lambda^2 \frac{p(t)}{v(t)} y_{k-1}(t) \right\} dt \quad (45)
 \end{aligned}$$

To start the initial process, the initial approximation given by $y_0(\xi)$ in eq. (45) can be expressed as follows:

$$y_0(\xi) = y(0) + y'(0)\xi + \frac{y''(0)}{2!} \xi^2 + \frac{y'''(0)}{3!} \xi^3 \quad (46)$$

where $y(0)$, $y'(0)$, $y''(0)$ and $y'''(0)$ are unknown constants that need to be found while applying the above dimensionless boundary condition (He, 1999).

The solution to eq. (44) can then be provided as

$$y(\xi) = \lim_{k \rightarrow \infty} y_k(\xi) \quad (47)$$

In order to obtain a reasonable approximate solutions, a large value of "n" is chosen instead of ∞ on the basis of accuracy required,

$$y(\xi) = y_n(\xi). \quad (48)$$

Substituting eq. (48) into the boundary condition, so that four systems of equations are obtained. This can be further assembled into matrix form

$$\begin{pmatrix} \ell_{11} & \ell_{12} & \ell_{13} & \ell_{14} \\ \ell_{21} & \ell_{22} & \ell_{23} & \ell_{24} \\ \ell_{31} & \ell_{32} & \ell_{33} & \ell_{34} \\ \ell_{41} & \ell_{42} & \ell_{43} & \ell_{44} \end{pmatrix} \begin{pmatrix} y(0) \\ y'(0) \\ y''(0) \\ y'''(0) \end{pmatrix} = \begin{pmatrix} 0 \\ 0 \\ 0 \\ 0 \end{pmatrix} \quad (49)$$

The coefficient matrix's determinant is zero for a non-trivial solution.

$$\begin{vmatrix} \ell_{11} & \ell_{12} & \ell_{13} & \ell_{14} \\ \ell_{21} & \ell_{22} & \ell_{23} & \ell_{24} \\ \ell_{31} & \ell_{32} & \ell_{33} & \ell_{34} \\ \ell_{41} & \ell_{42} & \ell_{43} & \ell_{44} \end{vmatrix} = 0 \quad (50)$$

Therefore, the numerical solution to the resulting polynomial in terms of (λ) for the dimensionless frequencies is provided. As a result, the natural frequencies are as follows:

$$\lambda = \frac{\mu}{l^2} \sqrt{\frac{E_0 I_0}{\rho_0 A_0}} \quad (51)$$

Numerical Implementation

To illustrate the methods proposed in this research, the free vibrations of axially FG spinning cantilever tapered Rayleigh beam is studied. In this section, the rotating Rayleigh beam is affixed at $x=0$ and its material parameters are assumed to be

$$\left. \begin{aligned} E(x)I(x) &= E(0)\left(1 + \beta\frac{x}{l}\right)I(0)\left(1 - c\frac{x}{l}\right)^{n+2} \\ \rho(x)A(x) &= \rho(0)\left(1 + \frac{x}{l} + \left(\frac{x}{l}\right)^2\right)A(0)\left(1 - c\frac{x}{l}\right)^n, \end{aligned} \right\} \quad (52)$$

where $\rho(0)$, $A(0)$, $I(0)$, and $E(0)$ represent mass per unit volume, cross-sectional area, moment of inertia, and Young's modulus at $x = 0$ respectively.

The centrifugal force $N(x)$ positioned at x distance from the center of rotation is expressed by

$$Q(x) = \int_x^l \rho(x)A(x)\Omega^2 x dx \quad (53)$$

where Ω is the rotational speed.

The case $n = 1$ is considered in eq. (40).

For example, the expression for $Q(x)$, $v(\xi)$, $q(\xi)$, $p(\xi)$ and $h(\xi)$ are given as follows:

$$Q(x) = \int_x^l \rho(\xi)A(\xi)\Omega^2 \xi d\xi \quad (54)$$

$$\begin{aligned} &= \int_x^l \rho(0)A(0)\left(1 - c\frac{\xi}{l}\right)\Omega^2 \xi d\xi \\ &= \rho(0)A(0)\Omega^2 l^2 \left[\frac{13}{12} - \frac{47c}{60} - \frac{\xi^2}{2} + \frac{(c-1)\xi^3}{3} + \frac{(c-1)\xi^4}{4} + \frac{c\xi^5}{5} \right] \end{aligned} \quad (55)$$

$$v(\xi) = \frac{E(x)I(x)}{E(0)I(0)} = \frac{E(0)I(0)\left(1 + \beta\frac{x}{l}\right)\left(1 - c\frac{x}{l}\right)^3}{E(0)I(0)} = (1 + \beta\xi)(1 - c\xi)^3 \quad (56)$$

$$q(\xi) = -\frac{Q(x)l^2}{E(0)I(0)} = -\alpha^2 \left[\frac{13}{12} - \frac{47c}{60} - \frac{\xi^2}{2} + \frac{(c-1)\xi^3}{3} + \frac{(c-1)\xi^4}{4} + \frac{c\xi^5}{5} \right] \quad (57)$$

$$p(\xi) = \frac{\rho(x)A(x)}{\rho(0)A(0)} = \frac{\rho(0)A(0)\left(1 + \frac{x}{l} + \left(\frac{x}{l}\right)^2\right)\left(1 - c\frac{x}{l}\right)}{\rho(0)A(0)} = (1 + \xi + \xi^2)(1 - c\xi) \quad (58)$$

$$h(\xi) = \frac{\rho(x)I(x)}{\rho(0)I(0)} = \frac{\rho(0)I(0)\left(1 + \frac{x}{l} + \left(\frac{x}{l}\right)^2\right)\left(1 - c\frac{x}{l}\right)^3}{\rho(0)I(0)} = (1 + \xi + \xi^2)(1 - c\xi)^3 \quad (59)$$

For free vibration, substitute eqs. (54) - (59) into eq. (14) to give

$$\begin{aligned} & \left[1 + (\beta - 3c)\xi + 3(c^2 - \beta c)\xi^2 + (3\beta c^2 - c^3)\xi^3 - \beta c^3\xi^4\right] \frac{d^4 y(\xi)}{d\xi^4} + 2\left[(\beta - 3c) + 6(c^2 - \beta c)\xi\right. \\ & \left. - 3(c^3 - 3\beta c^2)\xi^2 - 4\beta c^3\xi^3\right] \frac{d^3 y(\xi)}{d\xi^3} + 6\left[(c^2 - \beta c) - (c^3 - 3\beta c^2)\xi - 2\beta c^3\xi^2\right] \frac{d^2 y(\xi)}{d\xi^2} \\ & - \left[\frac{13}{12} - \frac{47c}{60} - \frac{\xi^2}{2} + \frac{(c-1)\xi^3}{3} + \frac{(c-1)\xi^4}{4} + \frac{c\xi^5}{5}\right] \alpha^2 \frac{d^2 y(\xi)}{d\xi^2} + \left[\xi - (c-1)\xi^2\right. \\ & \left. - (c-1)\xi^3 - c\xi^4\right] \alpha^2 \frac{dy(\xi)}{d\xi} + \gamma^2(\Lambda^2 + \alpha^2)\left[1 + (1-3c)\xi + (1-3c+3c^2)\xi^2\right. \\ & \left. - (3c-3c^2+c^3)\xi^3 + (3c^2-c^3)\xi^4 - c^3\xi^5\right] \frac{d^2 y(\xi)}{d\xi^2} + \gamma^2(\Lambda^2 + \alpha^2)\left[(1-3c)\right. \\ & \left. + 2(1-3c+3c^2)\xi - 3(3c-3c^2+c^3)\xi^2 + 4(3c^2-c^3)\xi^3 - 5c^3\xi^4\right] \frac{dy(\xi)}{d\xi} \\ & - \Lambda^2\left[1 - (c-1)\xi - (c-1)\xi^2 - c\xi^3\right] y(\xi) = 0 \end{aligned} \quad (60)$$

Applying the differential transform to eq. (60) gives

$$\begin{aligned} & \sum_{\ell=0}^k \left[\delta(k-\ell) + (\beta - 3c)\delta(k-\ell-1) + 3(c^2 - \beta c)\delta(k-\ell-2) + (3\beta c^2 - c^3)\delta(k-\ell-3)\right. \\ & \left. - \beta c^3\delta(k-\ell-4) \right] (\ell+1)(\ell+2)(\ell+3)(\ell+4)\bar{Y}(\ell+4) + 2\sum_{\ell=0}^k [(\beta - 3c)\delta(k-\ell) \\ & + 6(c^2 - \beta c)\delta(k-\ell-1) + 3(3\beta c^2 - c^3)\delta(k-\ell-2) - 4\beta c^3\delta(k-\ell-3)] (\ell+1)(\ell+2) \\ & (\ell+3)\bar{Y}(\ell+3) + 6\sum_{\ell=0}^k \left[(c^2 - \beta c)\delta(k-\ell) + (3\beta c^2 - c^3)\delta(k-\ell-1) - 2\beta c^3\delta(k-\ell-2) \right]. \end{aligned}$$

$$\begin{aligned}
 & (\ell+1)(\ell+2)\bar{Y}(\ell+2) - \sum_{\ell=0}^k \left[\left(\frac{13}{12} - \frac{47c}{60} \right) \delta(k-\ell) - \frac{1}{2} \delta(k-\ell-2) - \frac{(c-1)}{3} \delta(k-\ell-3) \right. \\
 & \left. + \frac{(c-1)}{4} \delta(k-\ell-4) + \frac{c}{5} \delta(k-\ell-5) \right] \alpha^2 (\ell+1)(\ell+2)\bar{Y}(\ell+2) + \sum_{\ell=0}^k [\delta(k-\ell-1) \\
 & - (c-1)\delta(k-\ell-2) - (c-1)\delta(k-\ell-3) - c\delta(k-\ell-4)] \alpha^2 (\ell+1)\bar{Y}(\ell+1) \\
 & + \gamma^2 (\Lambda^2 + \alpha^2) \sum_{\ell=0}^k [\delta(k-\ell) + (1-3c)\delta(k-\ell-1) + (1-3c+3c^2)\delta(k-\ell-2) \\
 & - (3c-3c^2+c^3)\delta(k-\ell-3) + (3c^2-c^3)\delta(k-\ell-4) - c^3\delta(k-\ell-5)] (\ell+1)(\ell+2)\bar{Y}(\ell+2) \\
 & + \gamma^2 (\Lambda^2 + \alpha^2) \sum_{\ell=0}^k [(1-3c)\delta(k-\ell) + 2(1-3c+3c^2)\delta(k-\ell-1) - 3(3c-3c^2+c^3)\delta(k-\ell-2) \\
 & + 4(3c^2-c^3)\delta(k-\ell-3) - 5c^3\delta(k-\ell-4)] (\ell+1)\bar{Y}(\ell+1) \\
 & = \lambda \sum_{\ell=0}^k [\delta(k-\ell) + (1-c)\delta(k-\ell-1) + (1-c)\delta(k-\ell-2) - c\delta(k-\ell-3)] \bar{Y}(\ell) \tag{61}
 \end{aligned}$$

Putting these values of $\bar{Y}(0) - \bar{Y}(3)$ and $k = 0$ into eq. (24), gives

$$\bar{Y}(4) = \frac{1}{24} \left[\left(\frac{415}{12} - 2\lambda\gamma^2 - 50\gamma^2 \right) s + 12z \right] \tag{62}$$

Putting the values of $\bar{Y}(0) - \bar{Y}(4)$ and $k = 1$ into eq. (24), gives

$$\bar{Y}(5) = \frac{1}{120} \left[\left(\frac{403}{4} - 2\lambda\gamma^2 - 50\gamma^2 \right) s + \left(\frac{599}{4} - 6\lambda\gamma^2 - 150\gamma^2 \right) z \right] \tag{63}$$

Putting the values of $\bar{Y}(0) - \bar{Y}(5)$ and $k = 2$ into eq. (24), yields

$$\begin{aligned}
 \bar{Y}(6) = & \frac{1}{360} \left[\left(\frac{245953}{576} + \lambda + \frac{505}{12} \lambda\gamma^2 - \frac{12625}{12} \gamma^2 + 50\lambda\gamma^4 + 625\gamma^4 + \lambda^2\gamma^4 \right) s \right. \\
 & \left. + \left(\frac{1461}{4} - \frac{21}{2} \lambda\gamma^2 - \frac{525}{2} \gamma^2 \right) z \right] \tag{64}
 \end{aligned}$$

Following the same recursive procedure, the m^{th} term $\bar{Y}(m)$ can be determined. Computer codes developed utilizing MAPLE 18, the natural frequencies and their related vibration modes were evaluated for $\gamma = 0.01$, $\beta =$

0.5, $\alpha = 5$ and $c = 0.5$ using eq. (61). The first four dimensionless frequencies are $\lambda_1 = 6.0321$ at $m = 32$, $\lambda_2 = 19.3552$ at $m = 33$, $\lambda_3 = 43.7817$ at $m = 38$ and $\lambda_4 = 79.8652$ at $m = 40$. Now to determine the first vibration mode, λ_1 is substituted into $\bar{Y}(0)$ to $\bar{Y}(32)$ and using eq. (22), the series function of the first vibration mode is obtained as

$$\begin{aligned}
 y_1(\xi)_{32} = & s(\xi^2 - 1.1203\xi^3 + 0.8803\xi^4 - 0.4649\xi^5 + 0.1501\xi^6 - 0.0234\xi^7 \\
 & - 0.0082\xi^8 + 0.0106\xi^9 - 0.0098\xi^{10} + 0.0058\xi^{11} - 0.0026\xi^{12} + 0.0011\xi^{13} - 0.0002\xi^{14} \\
 & + 0.0002\xi^{15} + 0.0001\xi^{16} + 3.6986 \times 10^{-5} \xi^{17} + 4.4152 \times 10^{-5} \xi^{18} + 1.2071 \times 10^{-5} \xi^{19} \\
 & + 1.1703 \times 10^{-5} \xi^{20} + 9.3479 \times 10^{-7} \xi^{21} - 1.1990 \times 10^{-7} \xi^{22} - 2.2572 \times 10^{-6} \xi^{23} \\
 & - 2.1389 \times 10^{-6} \xi^{24} - 1.9663 \times 10^{-6} \xi^{25} - 1.4513 \times 10^{-6} \xi^{26} - 1.0066 \times 10^{-6} \xi^{27} \\
 & - 6.2911 \times 10^{-7} \xi^{28} - 3.6291 \times 10^{-7} \xi^{29} - 1.8702 \times 10^{-7} \xi^{30} - 8.2063 \times 10^{-8} \xi^{31} \\
 & - 2.4896 \times 10^{-8} \xi^{32}) \tag{65}
 \end{aligned}$$

Similarly, the second vibration mode function is given by

$$\begin{aligned}
 y_2(\xi)_{33} = & s(\xi^2 - 1.5199\xi^3 + 0.6777\xi^4 - 0.9288\xi^5 + 0.6820\xi^6 - 0.1787\xi^7 + 0.1974\xi^8 \\
 & - 0.0740\xi^9 + 0.0393\xi^{10} - 0.0187\xi^{11} + 0.0040\xi^{12} - 0.0060\xi^{13} - 0.0025\xi^{14} - 0.0028\xi^{15} \\
 & - 0.0019\xi^{16} - 0.0013\xi^{17} - 0.0008\xi^{18} - 0.0004\xi^{19} - 0.0002\xi^{20} - 5.0658 \times 10^{-5} \xi^{21} \\
 & + 1.7332 \times 10^{-5} \xi^{22} + 4.6771 \times 10^{-5} \xi^{23} + 5.0368 \times 10^{-5} \xi^{24} + 4.3516 \times 10^{-5} \xi^{25} \\
 & + 3.2768 \times 10^{-5} \xi^{26} + 2.2504 \times 10^{-5} \xi^{27} + 1.4200 \times 10^{-5} \xi^{28} + 8.2466 \times 10^{-6} \xi^{29} \\
 & + 4.3338 \times 10^{-6} \xi^{30} + 1.9738 \times 10^{-6} \xi^{31} + 6.7339 \times 10^{-7} \xi^{32} + 3.7663 \times 10^{-8} \xi^{33}) \tag{66}
 \end{aligned}$$

Also, the third vibration mode function is given by

$$\begin{aligned}
 y_3(\xi)_{38} = & s(\xi^2 - 2.1222\xi^3 + 0.3637\xi^4 - 1.6178\xi^5 + 4.3493\xi^6 - 0.9556\xi^7 + 0.5350\xi^8 \\
 & - 1.9458\xi^9 + 0.1266\xi^{10} - 0.2244\xi^{11} + 0.4982\xi^{12} + 0.0080\xi^{13} + 0.0940\xi^{14} - 0.0510\xi^{15} \\
 & + 0.0065\xi^{16} - 0.0136\xi^{17} + 0.0038\xi^{18} - 0.0022\xi^{19} + 0.0009\xi^{20} - 0.0005\xi^{21} + 0.0001\xi^{22} \\
 & - 0.0001\xi^{23} + 1.9979 \times 10^{-5} \xi^{24} - 2.8957 \times 10^{-5} \xi^{25} + 3.3247 \times 10^{-6} \xi^{26} - 4.8826 \times 10^{-6} \xi^{27} \\
 & + 1.6778 \times 10^{-6} \xi^{28} + 7.0218 \times 10^{-8} \xi^{29} + 1.1225 \times 10^{-6} \xi^{30} + 5.9046 \times 10^{-7} \xi^{31} \\
 & + 5.9967 \times 10^{-7} \xi^{32} + 3.5216 \times 10^{-7} \xi^{33} + 2.5481 \times 10^{-7} \xi^{34} + 1.4333 \times 10^{-7} \xi^{35} \\
 & + 8.6733 \times 10^{-8} \xi^{36} + 4.3938 \times 10^{-8} \xi^{37} + 2.2159 \times 10^{-8} \xi^{38}) \tag{67}
 \end{aligned}$$

And the fourth vibration mode function is given by

$$\begin{aligned}
 y_4(\xi)_{40} = & s(\xi^2 - 2.8289\xi^3 - 0.0268\xi^4 - 2.3856\xi^5 + 16.0246\xi^6 - 6.7300\xi^7 - 3.5809\xi^8 \\
 & -14.7195\xi^9 + 7.5429\xi^{10} + 4.6064\xi^{11} + 8.0067\xi^{12} - 3.3188\xi^{13} - 2.3289\xi^{14} - 3.0214\xi^{15} \\
 & +0.5388\xi^{16} + 0.5239\xi^{17} + 0.7987\xi^{18} + 0.0425\xi^{19} - 0.0165\xi^{20} - 0.1256\xi^{21} - 0.0255\xi^{22} \\
 & -0.0162\xi^{23} + 0.0089\xi^{24} + 0.0014\xi^{25} + 0.0027\xi^{26} - 0.0004\xi^{27} + 0.0002\xi^{28} - 0.0002\xi^{29} \\
 & +2.5653 \times 10^{-5} \xi^{30} - 5.0620 \times 10^{-5} \xi^{31} + 9.0583 \times 10^{-6} \xi^{32} - 1.1038 \times 10^{-5} \xi^{33} \\
 & +1.7124 \times 10^{-6} \xi^{34} - 2.7800 \times 10^{-6} \xi^{35} + 2.4008 \times 10^{-7} \xi^{36} - 6.5664 \times 10^{-7} \xi^{37} \\
 & +5.8750 \times 10^{-8} \xi^{38} - 1.2516 \times 10^{-7} \xi^{39} + 3.3843 \times 10^{-8} \xi^{40}) \tag{68}
 \end{aligned}$$

By going through similar recurrence process, other higher order dimensionless frequencies (λ_5 , λ_6 , λ_7 and λ_8) and the vibration mode functions that correspond to them can be found.

Results

Table 1. The first four dimensionless frequencies' convergence for different number of terms (m)

m	λ_1	λ_2	λ_3	λ_4
6	4.3365	359.8506	-	-
7	6.8139	41.2999	-	-
8	6.7090	39.5918	-	-
9	5.8981	24.8219	-	-
10	6.5596	25.1675	73.8991	-
11	5.9982	22.2744	59.7463	286.4150
12	6.2251	22.1913	44.0790	169.7176
13	6.0818	21.1222	43.6837	94.3844
14	6.1014	20.6995	40.6594	76.8238
15	6.0674	20.1954	42.7924	59.8628
16	6.0525	19.8467	42.0666	58.3962
17	6.0439	19.5660	44.1464	54.3939
18	6.0319	19.3523	43.1897	182.9810
19	6.0278	19.2103	43.8660	131.3620
20	6.0227	19.1222	43.5082	106.9456

21	6.0218	19.0877	43.7660	84.3971
22	6.0215	19.0911	43.6877	79.6413
23	6.0228	19.1224	43.7781	76.1763
24	6.0246	19.1675	43.7624	78.0626
25	6.0265	19.2159	43.7898	78.4507
26	6.0283	19.2597	43.7861	80.4262
27	6.0298	19.2950	43.7923	80.0230
28	6.0308	19.3208	43.7898	80.2573
29	6.0315	19.3379	43.7896	79.9285
30	6.0318	19.3480	43.7875	79.9670
31	6.0320	19.3532	43.7861	79.8778
32	6.0321	19.3551	43.7846	79.8958
33	6.0321	19.3552	43.7837	79.8707
34	6.0321	19.3551	43.7828	79.8751
35	6.0320	19.3550	43.7823	79.8670
36	6.0320	19.3549	43.7820	79.8678
37	6.0319	19.3548	43.7818	79.8654
38	6.0319	19.3499	43.7817	79.8656
39	6.0319	19.3498	43.7817	79.8651
40	6.0319	19.3497	43.7816	79.8652

Table 2. The Convergence of the fifth-eighth dimensionless frequencies for different number of terms (m)

m	λ_5	λ_6	λ_7	λ_8
20	263.2267	-	-	-
25	100.0973	169.7261	384.3374	1033.7109
26	97.2986	143.2639	291.7822	705.7031
27	110.4462	115.0735	234.0915	511.3601
28	190.3831	393.6437	921.2227	2333.7308
29	161.9919	310.7301	673.2418	1695.1102
30	136.2866	255.0703	513.8866	1173.6024

40	127.6035	186.1657	285.4292	473.6117
41	127.6078	182.6694	253.6838	406.5400
42	127.5966	183.7248	230.2007	354.4214
43	127.5989	185.2632	220.4645	312.4231
44	127.5952	186.8228	219.7709	280.0039
45	127.5952	187.1176	232.1961	250.4475
46	127.5938	187.1295	340.5123	528.1634
47	127.5936	186.9677	306.3635	464.0827
48	127.5931	186.9140	274.1329	412.4063
49	127.5930	186.8753	257.2678	369.8167
50	127.5929	186.8745	253.7965	335.5048
51	127.5928	186.8712	254.5790	310.2504
52	127.5928	186.8733	256.1257	299.6250
53	127.5928	186.8725	257.4041	300.1089
54	127.5928	186.8726	257.7453	314.1927
55	127.5928	186.8721	257.7446	432.1762
56	127.5928	186.8720	257.6346	393.1672
57	127.5928	186.8718	257.5810	358.7274
58	127.5928	186.8717	257.5541	339.6246
59	127.5928	186.8716	257.5515	336.3390
60	127.5928	186.8716	257.5512	336.9179
64	127.5928	186.8716	257.5532	339.5808
65	127.5928	186.8716	257.5531	339.5070
66	127.5928	186.8716	257.5530	339.4631
67	127.5928	186.8716	257.5530	339.4441
68	127.5928	186.8716	257.5530	339.4413
69	127.5928	186.8716	257.5530	339.4418
70	127.5928	186.8716	257.5530	339.4431
71	127.5928	186.8716	257.5530	339.4437
72	127.5928	186.8716	257.5530	339.4438

Table 3. Comparison of the first eight dimensionless frequencies for $\gamma = 0.01$, $\beta = 0.5$, $\alpha = 5$

and $c = 0.5$

λ_i	DTM	VIM
λ_1	6.0319	6.0319
λ_2	19.3496	19.3496
λ_3	43.7817	43.7817
λ_4	79.8656	79.8656
λ_5	127.5928	127.5928
λ_6	186.8716	186.8716
λ_7	257.5529	257.5529
λ_8	339.4437	339.4437

Table 4. Effects of the inverse of slenderness ratio (γ), rotational speed (α) and taper ratio (c) on the dimensionless frequencies

γ	α	λ_1			λ_2			λ_3		
		$c = 0.25$	$c = 0.50$	$c = 0.75$	$c = 0.25$	$c = 0.50$	$c = 0.75$	$c = 0.25$	$c = 0.50$	$c = 0.75$
0.100	0	2.4134	2.5528	2.8205	14.6015	13.4591	12.0316	37.0061	33.4240	28.5018
0.050		2.4233	2.5653	2.8347	15.4831	14.0155	12.3341	42.3919	36.8903	30.3118
0.033		2.4252	2.5677	2.8375	15.6636	14.1262	12.3926	43.6754	37.6600	30.6863
0.025		2.4258	2.5685	2.8384	15.7282	14.1655	12.4133	44.1531	37.9410	30.8207
0.020		2.4261	2.5689	2.8388	15.7583	14.1839	12.4228	44.3796	38.0733	30.8835
0.013		2.4264	2.5693	2.8392	15.7883	14.2020	12.4324	44.6068	38.2053	30.9458
0.010		2.4265	2.5694	2.8394	15.7988	14.2084	12.4357	44.6871	38.2518	30.9678
BE		2.4267	2.5696	2.8396	15.8123	14.2166	12.4400	44.7910	38.3119	30.9961
0.100		5	5.8582	5.9707	6.1913	19.2050	18.2647	17.0030	41.3885	38.1579
0.050	5.8950		6.0169	6.2412	20.4468	19.0709	17.4621	47.5577	42.1971	35.7921
0.033	5.9020		6.0255	6.2505	20.7002	19.2308	17.5508	49.0268	43.0930	36.2416
0.025	5.9044		6.0286	6.2537	20.7909	19.2877	17.5821	49.5735	43.4201	36.4027
0.020	5.9056		6.0300	6.2552	20.8332	19.3141	17.5967	49.8326	43.5740	36.4781
0.013	5.9067		6.0314	6.2567	20.8752	19.3404	17.6111	50.0926	43.7276	36.5530
0.010	5.9071		6.0318	6.2572	20.8899	19.3496	17.6161	50.1845	43.7817	36.5793
BE	5.9076		6.0325	6.2579	20.9089	19.3614	17.6226	50.3034	43.8516	36.6132
0.100	10		10.7223	10.8187	11.0224	28.8205	28.0700	26.7615	52.0128	49.5234
0.050		10.7882	10.9057	11.1203	30.7782	29.3438	27.5044	60.1575	54.9368	48.5590
0.033		10.8010	10.9220	11.1386	31.1770	29.5965	27.6478	62.0932	56.1352	49.1769
0.025		10.8055	10.9277	11.1449	31.3196	29.6862	27.6985	62.8131	56.5726	49.3985
0.020		10.8075	10.9303	11.1479	31.3862	29.7280	27.7220	63.1545	56.7783	49.5021
0.013		10.8096	10.9330	11.1508	31.4523	29.7695	27.7453	63.4967	56.9837	49.6049
0.010		10.8103	10.9339	11.1519	31.4755	29.7840	27.7535	63.6178	57.0560	49.6411
BE		10.8113	10.9350	11.1532	31.5054	29.8027	27.7640	63.7743	57.1495	49.6877

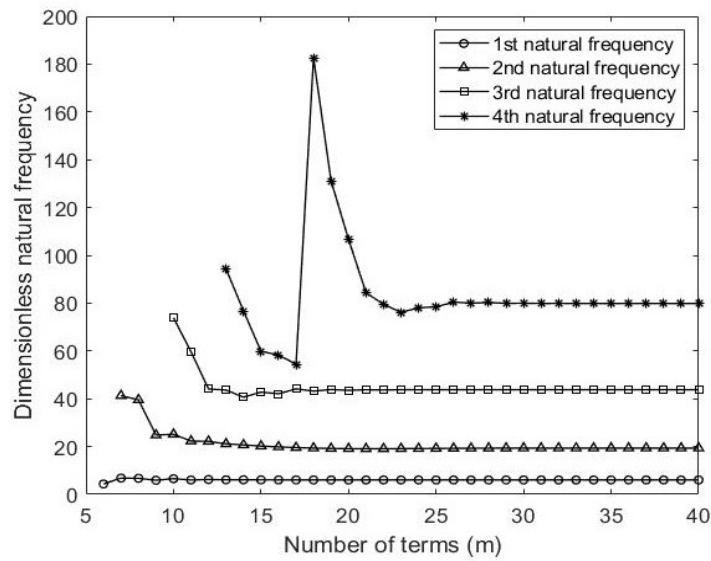


Figure 2: The convergence of the first, second, third and fourth dimensionless frequencies

$$(\lambda_1 = 6.0321, \lambda_2 = 19.3552, \lambda_3 = 43.7817, \lambda_4 = 79.8652)$$

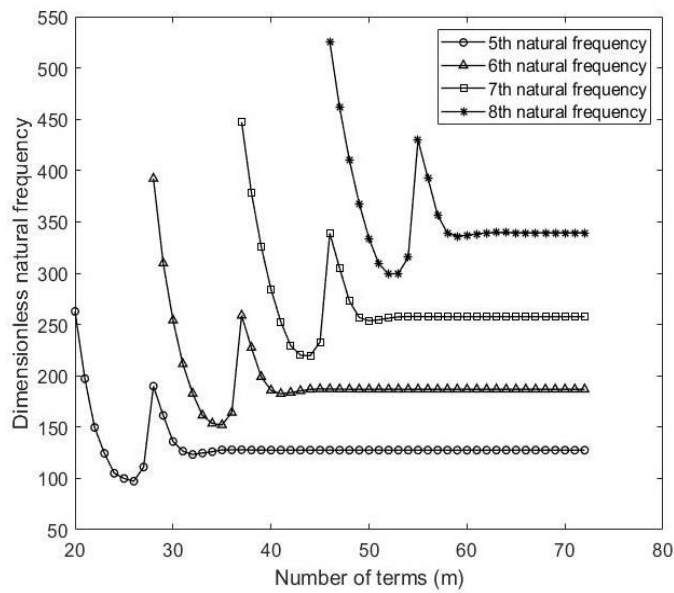


Figure 3: The convergence of the fifth, sixth, seventh and eighth dimensionless frequencies

$$(\lambda_5 = 127.5952, \lambda_6 = 186.8726, \lambda_7 = 257.5531, \lambda_8 = 339.4438)$$

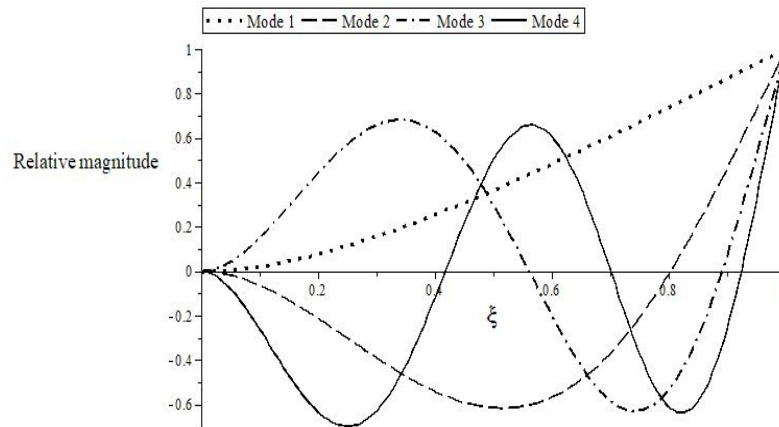


Figure 4: The first, second, third and fourth vibration modes

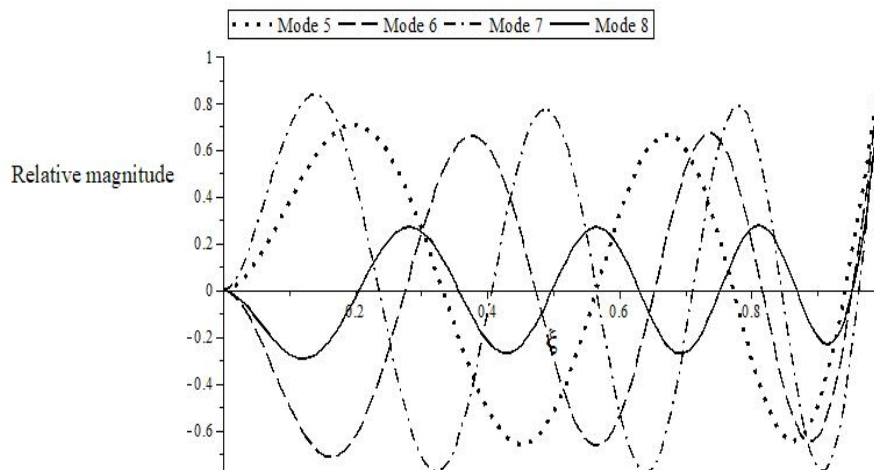


Figure 5: The fifth, sixth, seventh and eighth vibration modes

Discussion

Figures 2 and 3 (obtained using Tables 1 and 2) show the trend in the convergences of the initial eight dimensionless frequencies of an axially FG rotating cantilever tapered Rayleigh beam. It was noted that as the number of terms (m) increases, the first eight dimensionless frequencies λ_1 to λ_8 converged to 6.0321, 19.3552, 43.7817, 79.8652, 127.5952, 186.8726, 257.5531 and 339.4438 one after the other without skipping any frequencies for $\epsilon = 0.0001$, the corresponding number of terms (m) are 32, 33, 38, 40, 45, 54, 65 and 72 respectively (see Tables 1 and 2). It was noted that the first dimensionless frequency λ_1 needed 32 terms to reach exact solution, second dimensionless frequency λ_2 used 33 terms, third dimensionless frequency λ_3 needed 38 terms to reach exact solution while the fourth dimensionless frequency λ_4 took 40 terms to reach the convergence point and so on, as shown in Table 1 and 2, as well as Figures 2 and 3. Figures 4 and 5 show the dynamical behaviour of axially functionally graded rotating cantilever tapered Rayleigh beam at different dimensionless frequencies, thereby leading to various vibration modes. In particular, the first four vibration modes for example, are determined using their associated dimensionless frequencies and equations (65) - (68) respectively.

Likewise, the other higher-order vibration modes were determined using their respective dimensionless frequencies and the associated vibration mode functions.

Table 3 presents a comparison of the dimensionless frequencies computed using the differential transform method and the variational iteration method, showing that both methods produce identical results. Table 4 shows the findings for the initial three dimensionless frequencies λ for varied values of inverse of the slenderness ratio γ , for three distinct values of the tapered ratio c and different values of the rotational speed α . It was observed that the rotational speed has an increasing effect on the dimensionless frequencies, as the inverse of slenderness ratio increases, there was a decrease in the dimensionless frequencies. As the taper ratio rises, the dimensionless frequencies, excluding the fundamental ones, tend to decrease. However, the fundamental dimensionless frequencies show a slight increase with increasing taper ratio, as evident from the data in Table 4. This indicates that the fundamental frequencies exhibit an opposite trend compared to the higher-order frequencies. The key findings indicate that increasing the rotational speed of an axially functionally graded rotating clamped-free tapered Rayleigh beam results in higher dimensionless frequencies, while increasing the inverse of slenderness ratio yields a reduction in its dimensionless frequencies. Additionally, increasing the beam's taper ratio generally causes a reduction in its dimensionless frequencies.

Conclusion

Using the methods proposed in this work, closed-form series solutions for natural vibration problem of an axially FG rotating cantilever tapered Rayleigh beam were obtained. By comparing the DTM and the VIM, both methods are easy and effective in calculating the dimensionless frequencies with high accuracy and convergence rate. The first eight dimensionless frequencies and the vibration modes are calculated and plotted. The DTM and VIM processes are simple and easy to follow. All the algebraic calculations are executed speedily by using MAPLE 18. A comparison between the results of the two methods are carried out and are found to be consistent. Thus, this study demonstrated the vibration analysis of FG rotating cantilever tapered Rayleigh beams is performed with high computational efficiency and precision using DTM and VIM.

Recommendation

The study on free vibration analysis of axially functionally graded rotating cantilever tapered Rayleigh beams can be extended by incorporating nonlinear vibration effects, temperature-dependent material properties, aerodynamic influences, and FG plates and shells under rotation will further broaden its engineering applications. Methodological improvements can be made by developing hybrid numerical methods, applying artificial intelligence and machine learning techniques, and conducting experimental validation to verify theoretical findings. Additionally, investigating different tapering profiles, axial forces, rotational speeds, and material gradation patterns can optimize structural performance. The findings of this study could be relevant in the fields of mechanical engineering by designing lightweight materials with optimized vibration properties, in aerospace engineering by minimizing vibration of spacecraft structures while maintaining the strength and efficiency, and in structural dynamics by having an understanding of how slender beams response to external forces and vibrations.

References

- Abu-Alshaikh, I.M., & Almbaidin, A.A., (2020). Analytical responses of functionally graded beam under moving mass using Caputo and Caputo–Fabrizio fractional derivative models. *Journal of Vibration and Control*, 26(19-20), 1859-67. doi:10.1177/1077546320908103
- Akbaş S.D., (2020). Forced vibration responses of axially functionally graded beams by using Ritz method. *Journal of Appl. Comput. Mech.*, doi: 10.22055/JACM.2020.34865.2491
- Al-Hawamdeh O., Abu-Alshaikh I., & Al-Huniti N., (2017). Finite element coding of functionally graded beams under various boundary and loading conditions. *Journal of Applied Research on Industrial Engineering*, 4(4), 279–90.
- Anjum, N., Raheed, A., He., J.H., & Alsolami, A.A., (2024). Free vibration of a tapered beams by the Aboodh Transform-based Variational Iteration Method. *Journal of Computational Applied Mechanics*, 55(3), 440-550.
- Avcar, M., & Alwan, H. H. A. (2017). Free vibration of functionally graded Rayleigh beam. *International Journal of Engineering and Applied Sciences*, 9(2), 127-137.
- Banerjee, J.R., (2019). Review of the dynamic stiffness method for free-vibration analysis of beams. *Transportation Safety and Environment*, 1(2), 106–16.

- Chen, Y., Liu H., Xian, G., Zhang, D., Li L., & Li J., (2024). Theoretical modeling and dynamic analysis of a rotating piezoelectric laminated beam with setting angles. *Applied Mathematical Modelling*, 130, 635-57.
- Dhar, D., & Sakar S., (2023). Free vibration analysis of rotating cantilever beam using P-type Finite Element Method. *Proceedings of the ASME Aerospace Structures, Structural Dynamics, and Materials Conference*, <https://doi.org/10.1115/SSDM2023-108468>.
- Ebrahimi F., & Dashti S., (2015). Free vibration analysis of a rotating non-uniform functionally graded beam. *Steel and Composite Structures*, 19(5), 1279-98.
- Gbadeyan, J.A., & Olotu O.T., (2020). Natural vibration analysis of a tapered rotating prestressed Rayleigh beam using differential transform method. *FUTA Journal of Engineering and Engineering Technology*, 14(2), 207 – 30.
- Guo, X., Su, Z., & Wang, L., (2024). Dynamic characteristics of multi-span spinning beams with elastic constraints under an axial compressive force. *Appl. Math. Mech. Engl. Ed.*, 45, 295–310, <https://doi.org/10.1007/s10483-024-3082-9>
- He, J.H., (1999). Variational Iterational method - a kind of non-linear analytical technique: Some examples. *Int. Journal of Non-linear Mechanics*, 34(4), 699–708.
- Huang, J., Zhou, K., Xu J., Wang H., & Song H., (2023). Flap-wise vibrations of non-uniform rotating cantilever beams. An investigation with operational experiments. *Journal of sound and vibration*, 553, 1-13.
- Huang, Y., Liu H., & Zhao. Y., (2023). Dynamic Analysis of Non-Uniform Functionally Graded Beams on Inhomogeneous Foundations Subjected to Moving Distributed Loads. *Applied Sciences*, 13(18), 10309. <https://doi.org/10.3390/app131810309>
- Ilechukwu, A.E., Omenyi S., Abonyi. S.E., Okafor, A.A., & Odeh, C.P., (2024). Theoretical and Simulation Finite Element Modal Analysis of Rotating Cantilever Beam. *International Journal of Research and Innovation in Applied Sci.*, 10(2), 291-306. DOI: 10.51584/IJRIAS.2024.90225
- Kumar, P.R., Mohana K.M., & Rao N.M., (2017). Free vibration analysis of functionally graded rotating beam by differential transform method. *Indian Journal of Engineering and Materials Sci.*, 24, 104-14.
- Lee, J.W., (2017). Free vibration analysis of functionally graded Bernoulli-Euler beams using an exact transfer matrix expression. *Int. Journal of Mechanical Sci*, 122, 1-17.
- Li, X.F., Tang, A.Y., Wu, J.X., & Lee, K.Y., (2015). Bending vibration of rotating tapered cantilevers by integral equation method. *AIAA*, 49, 872-876.
- Nguyen D.K., Vu A., Le N., & Pham V.N., (2020). Dynamic behavior of a bidirectional functionally graded sandwich beam under non-uniform motion of a moving load. *Shock and Vibration*, Article ID 8854076, <https://doi.org/10.1155/2020/8854076>
- Ozdemir, O. (2019). Vibration analysis of rotating timoshenko beams with different material distribution properties. *Journal of Eng. Sci. Tech.*, 7(2), 272-86.
- Padhi, S.N., Raghu-Ram, K.S., Babu, J.K., & Rout T., (2019). Characterization of functionally graded Timoshenko beams with variable rotational speed. *Int. Journal of Recent Tech. and Eng.*, 8(4), 2277-3878
- Taima, M.S., Shehab, M.B., El-Sayed, T.A., & Friswell, M.I., (2023). Comparative study on free vibration analysis of rotating bi-directional functionally graded beams using multiple beam theories with uncertainty considerations. *Sci Rep.* 2023, 13, 17917, <https://doi.org/10.1038/s41598-023-44411-0>
- Wang, L, Su Z., & Wang L., (2022). Inplane vibration analysis of rotating beams with elastic restraints. *Journal of Sound and Vibration*, 29(7-8), <https://doi.org/10.1177/10775463211064690>
- Zhou, J.K. (1986). Differential transformation and its applications for electrical circuits. *Huazhong University Press, Wuhan, China*, 1986.